Effects of Ultraviolet and Electron Radiations on Graphite-Reinforced Polysulfone and Epoxy Resins

C. GIORI * and T. YAMAUCHI, *IIT Research Institute, Chicago, Illinois 60616*

Synopsis

Degradation mechanisms have been investigated for graphite/polysulfone and graphite/epoxy laminates exposed to ultraviolet and high-energy electron radiations in vacuum up to 960 equivalent sun hours and 10^9 rads, respectively. Based on GC and combined GC/MS analysis of volatile by-products evolved during irradiation, several free radical mechanisms of composite degradation have been identified. All the composite materials evaluated have shown high electron radiation stability and relatively low ultraviolet stability as indicated by low G values and high quantum yields for gas formation. Mechanical property measurements of irradiated samples did not reveal significant changes, with the possible exception of UV exposed polysulfone laminates. Hydrogen and methane have been identified as the main byproducts of irradiation, along with unexpectedly high levels of CO and CO_2. Initial G values for methane relative to hydrogen formation are higher in the presence of isopropylidene linkages, which occur in bisphenol-A based resins.

INTRODUCTION

Composite materials offer substantial advantages over conventional metallic materials for large space system applications due to their superior strength and stiffness-to-weight ratios and their low coefficient of thermal expansion. The major problem in utilizing composites for satellite structural applications is the degradation of material properties under the effect of the vacuum-radiation environment of space. Long-term stability at geosynchronous orbit is of primary concern. The use of composite materials for large geostationary structures presents a number of uncertainties because of the lack of information on the effects of thermal cycling, high vacuum, and space radiation. Spacecrafts in synchronous earth orbit are periodically eclipsed from the sun by the earth. This may produce a significant thermal shock effect on the composite. Vacuum may cause outgassing and migration of low molecular weight components from the matrix material. Another critical problem is the degradation of the composite matrix under the effect of radiation. This problem is particularly complex because of the nature of the geosynchronous radiation environment and the requirement for stability to ultraviolet as well as high energy radiations. Protection against heat and ultraviolet radiation may be afforded by the use of thermal control coatings. Such coatings, however, add undesired weight to the composite structure and do not provide protection against penetrating radiations such as high energy electrons.

* Present address: Borg-Warner Chemicals, Inc., Wolf and Algonquin Roads, Des Plaines, Ill. 60018.

Journal of Applied Polymer Science, Vol. 29, 237–249 (1984)
 CCC 0021-8995/84/010237-13$04.00

An understanding of the radiation behavior of composite materials is required in order to predict their long-term durability in a space environment. A knowledge of the degradation process is necessary for predicting the long-term behavior based on short-term exposure data, as well as for correlating accelerated exposure data with real time material performance. The main objective of this study is to establish the mechanisms of degradation and predict the long-term durability of graphite-reinforced composites, including epoxies and polysulfone matrix materials. These resins have shown the greatest potential for satellite structural applications.

EXPERIMENTAL

Materials

The matrix resins utilized for this study are (a) polysulfones and (b) epoxy resins of high functionality. The polysulfone evaluated in this work is P1700 (Union Carbide Corp.), which is the product of condensation of bisphenol-A with 4,4′-dichlorodiphenylsulfone:

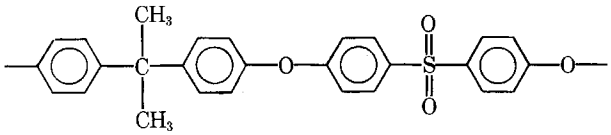

The epoxies used as matrix materials are high temperature resins based on the tetraglycidyl derivative of methylenedianiline, commercially available under the trade name MY720 (Ciba-Geigy Corp.):

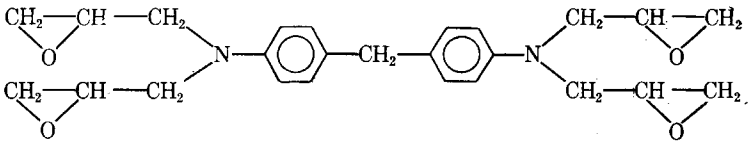

The high functionality of this resin results in a high degree of crosslinking and high heat distortion temperature of the cured product. The hardener utilized in conjunction with MY720 is 4,4′-diaminodiphenylsulfone (DDS):

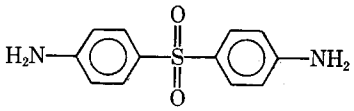

Two commercial epoxy resins based on MY720 and DDS have been evaluated, Fiberite 934 and Narmco 5208. Narmco 5208 contains also a minor amount of a bisphenol-A-based resin. Graphite fibers utilized for the fabrication of laminates are C6000 (Celanese Corp.) and T300 (Hercules, Inc.). Ultraviolet and high-energy electron exposure tests have been conducted on four-ply, unidirectional graphite laminates of polysulfone P1700/C6000 and two epoxy systems: Fiberite 934/T300 and Narmco 5208/T300. Fiber volume contents of the laminates and % resin by weight are given in Table I.

TABLE I
Fiber/Resin Content of Graphite Laminates

Material	Resin density	Fiber density	Vol % fiber	Wt % resin
P1700/C6000	1.3	1.76	47.9	44.5
934/T300	1.3	1.75	47.5	45.1
5208/T300	1.3	1.75	60.3	32.8

Apparatus for Sample Irradiation

The systems used for ultraviolet exposure consisted of 38 mm diam, 305 mm long quartz tubes sealed on stainless steel and equipped with 70 mm CFF flanges and ultrahigh vacuum valves. For electron irradiation, Pyrex tubes of the same size and valves with gold seals were employed. These vacuum assemblies allow gas collection for GC and GC/MS analysis of volatile byproducts evolved from the sample during radiation exposure. The exposure tubes containing the composite samples were dried at 120°C overnight under reduced pressure. The tubes were subsequently evacuated to 10^{-7} torr or less using an ion pump. For electron irradiation, tube assemblies were equipped with a copper–constantan thermocouple to monitor sample temperature variations during electron exposure.

Radiation Sources and Conditions

Ultraviolet Exposure Tests

The ultraviolet radiation source was a A-H6 high pressure, quartz-jacketed, water-cooled mercury-arc lamp. Its radiation energy is emitted mainly in a broad continuum spreading all the way down to below 230 nm. Its high ratio of ultraviolet-to-total energy allows accelerated ultraviolet testing at several equivalent solar factors. Ultraviolet exposure tests were conducted using a space ultraviolet acceleration factor of 4, which is equivalent to an ultraviolet flux of 0.7 cal/cm^2·min in the wavelength region 200–400 nm. The following ultraviolet exposure doses were utilized: 210, 480, 720, and 960 equivalent sun hours (ESH).

High Energy Electron Exposure Tests

The electron linear accelerator of IRT Corp. was utilized for high energy electron exposure. This system can provide electron beams over a wide range of energies. The samples were irradiated at a mean dose rate of 10.8 krad/s. Although dose rates as high as 50 krad/s could be achieved, a lower dose rate was employed to prevent an excessive temperature increase of the samples. At the dose rate employed, the irradiated samples reached a maximum temperature of 49°C. Total doses of 5×10^7, 1×10^8, 5×10^8, and 1×10^9 rads were utilized. The accelerator was tuned to provide a 12 MeV beam with an average pulse current of 575 μA, a pulse width of 6 μs, and a repetition rate of 180 Hz. The beam was rastered across the sample area with an IRT magnetic coil deflection unit.

Gas Analysis

GC Analysis

After irradiation, the sample tube assembly was attached to the vacuum line, filled with zero-grade helium, and the gases were allowed to mix for 1 h prior to analysis. An irradiated blank was run through the analysis procedure. Traces of H_2 and CO_2 were identified as impurities present in the helium used to fill the sample tube, and deducted from the results.

Analysis of SO_2. SO_2 analysis was conducted using a gas chromatograph fitted with a sulfur-specific flame photometric detector. Separation was accomplished using a 254 × 3 mm stainless steel column packed with Porapak QS. The analysis was run isothermally at 180°C. Helium was used as a carrier gas. Wall absorption of SO_2 complicated the analysis and made SO_2 quantification uncertain.

Analysis of H_2, CH_4, CO, and CO_2 and Low Molecular Weight Hydrocarbons. H_2, CH_4, CO, and hydrocarbons up to C_3 were analyzed using a trace gas analyzer equipped with a helium ionization detector. For H_2 and CO analysis the analyzer was fitted with 50 × 3 mm stainless steel column packed with 100/120-mesh molecular sieve 5A. Helium carrier gas flow was set at 30 ml/min and the analysis was run isothermally at 100°C. CH_4, CO_2, and hydrocarbon analysis was accomplished by fitting the instrument with 254 × 3 mm column packed with 100/120-mesh Porapak QS. Helium flow was set at 30 mL/min and the analysis run isothermally at 40°C for CO_2 and CH_4 and isothermally at 150°C for higher hydrocarbons. The sample was injected via an 8.9-mL sample loop attached to both the trace Gas analyzer and a standard vacuum line. This setup allows the sample loop to be evacuated, filled with sample at a known pressure, and injected without danger of contamination due to atmospheric gases. The instrument was calibrated using standard gas mixtures.

GC/MS Analysis

For GC/MS analysis, the remaining gas sample from the irradiated polymer tube was collected in a cryogenic trap. The rate of sample withdrawal and collection was controlled with a needle valve situated between the trap and the vacuum system. Upon termination of the collection procedure, the trap was filled with UHP He to ambient pressure, removed from the collection apparatus, and attached to the injection port of the GC. By rapidly heating the trap (up to 250°C), while reverse-flushing with helium carrier gas for 1 min, the sample was injected directly onto the GC column for analysis. A 50 m × 0.05 mm I.D. OV-101 SCOT column was used, with a carrier gas flow rate of 3.0 mL/min and an injector split ratio of 10:1. The column was held initially at a temperature of 35°C for 10 min, and then programmed at 4°C/min to 210°C. The total column effluent was coupled directly to a double-focusing mass spectrometer operated at low resolution. The ion source of the mass spectrometer consists of a combination of a standard electron impact source and an electron impact ionization detector (EID). By operating the EID at low electron energy, the carrier-gas-free total ion current signal from the GC could be monitored in real-time using a strip chart recorder.

Because of the complexity of the samples in the present investigation, extensive

use of standards throughout the elution range was obviously impractical. To obtain an estimate of the amount of each particular component present in the sample, the MS response factor for known amounts of a standard (*n*-decane) was established. This factor was then used to determine the amount of each substance of interest in terms of *n*-decane, by direct conversion of the peak areas.

RESULTS AND DISCUSSION

UV and Electron Exposure Studies

Results of GC analysis of volatile byproducts evolved during irradiation can be generally interpreted in terms of free radical processes involving several bonds in the polymer structures. Although the primary process of electron radiation damage involves ionization, subsequent steps leading to chain scission and crosslinking, with concurrent gas formation, take place by free radical mechanisms. This explains the similarity of the products obtained by ultraviolet and electron irradiation.

Formation of H_2, CH_4, and C_2H_6 can be explained in terms of cleavage of C—C and C—H bonds at the isopropylidene unit followed by free radical quenching via H or CH_3 abstraction. These mechanisms are expected to take place with P1700/C6000. To some extent, these mechanisms may also apply to Narmco 5208, which contains a small percentage of a bisphenol-A resin. For Fiberite 934, that does not contain bisphenol-A, the glycidyl groups of MY720 are believed to be mainly responsible for the formation of hydrogen and low molecular weight hydrocarbons.

Initial G values and quantum yields for gas formation are reported in Table II. Initial values are more significant than average values, since the gas evolved from the samples is retained in the exposure tubes and may undergo further reactions. Gas yields were calculated as moles produced per square centimeter of irradiated sample (in the case of ultraviolet exposure) or per gram of irradiated resin (in the case of electron exposure). This allows direct comparison of gas yields for different materials, since the resin content of the three laminates was different and the sample size was also slightly different. It is interesting to compare the G values for H_2 and CH_4 for the three laminates tested. These G values can be related to the presence of isopropylidene units (bisphenols-A) in the matrix resins, and show that methane is more readily formed when bisphenol-A is present due to the energetically favored elimination of CH_3 radicals from the isopropylidene units followed by hydrogen abstraction. (Hydrogen abstraction is favored over CH_3 radical recombination, as indicated by the fact that yield of methane is always higher than that of ethane.) The concentration of isopropylidene units (due to bisphenol-A) decreases in order P1700 > 5208 > 934. In the same order, G_{H_2} increases (from 9.3 to 24.9 to 48.6 $\times 10^{-3}$) and G_{CH_4} decreases (from 2.1 to 0.13 to 0.11 $\times 10^{-3}$). However, this trend is not apparent for the quantum yields of ultraviolet exposed samples.

With the exception of the oxides of carbon, H_2 is by far the predominant product of electron irradiation (on a molar basis), particularly in the case of Fiberite 934 and Narmco 5208, for which G_{CH_4} is low. In the case of ultraviolet irradiation, H_2 and CH_4 are both important products.

TABLE II
Initial Quantum Yields and G Values for Main Gas Formation

	Initial quantum yields[a] ($\times 10^3$)			Initial G values[b] ($\times 10^3$)		
Product	P1700/C6000	934/T300	5208/T300	P1700/C6000	934/T300	5208/T300
H_2	0.20	0.037	1.11	9.3	48.6	24.9
CH_4	0.078	0.18	0.33	2.1	0.11	0.13
C_2H_6	0.01	0.05	0.11	0.042	0.012	$<10^{-3}$
C_3H_8	0.027	0.013	0.025	0.028	0.0045	$<10^{-3}$
CO	1.90	1.47	3.26	10.5	3.1	23.0
CO_2	1.57	0.92	0.66	6.1	3.9	80.8
C_6H_6	0.002	0.0015	0.026	0.0034	$<10^{-3}$	$<10^{-3}$
SO_2	Not measured	Not measured	0.0027	0.014	Not measured	Not measured
Total	3.79	2.67	5.52	28.1	55.7	128

[a] Molecules formed per photon absorbed in the ultraviolet region. Calculations based on a quantum flux of 1.327×10^{-10} Einsteins/s·cm^2 in the 200–400 nm range.

[b] Molecules formed per 100 eV absorbed. Only the polymer portion of the laminates has been taken into account for the calculations.

High yields of CO and CO_2 have been found for all samples exposed to ultraviolet and electron irradiation. Likewise, high yields of CO and CO_2 have been reported by Gesner and Kelleher[1] for ultraviolet irradiation of polysulfone in a vacuum. Formation of CO can be ascribed to decarbonilation reactions. Formation of CO_2 in relatively high yields is surprising. Formation of CO_2 would be expected under photooxidative conditions, but in a vacuum it cannot be readily explained. Presence of carboxylated groups formed by oxidation during processing is a possible explanation. In the case of Narmco 5208 exposed to electron irradiation, the rate of CO_2 formation was unusually high.

Possible oxidative mechanisms leading to CO_2 formation may arise from oxygen formed by the decomposition of SO_2. SO_2 can result from the cleavage of C—S bonds. SO_2 is known to decompose photochemically and radiochemically according to the following mechanisms[2]:

$$SO_2 \begin{cases} \nearrow SO + \tfrac{1}{2}O_2 \\ \searrow \tfrac{1}{2}SO + \tfrac{1}{2}SO_3 \end{cases}$$

Sulfur monoxide rapidly disproportionates to sulfur and SO_2; likewise, SO_3 decomposes photochemically to SO_2 and O_2:

$$2SO \rightarrow S + SO_2$$

$$SO_3 \rightarrow SO_2 + \tfrac{1}{2}O_2$$

SO_2 quantification was not positively achieved in this study mainly due to wall absorption and retention of the polar SO_2. However, the available data indicates that SO_2 is not a major product of UV and electron exposure. Relatively low values for SO_2 formation have been reported by Davis et al.[3] for electron irradiation and by Gesner and Kelleher[1] for ultraviolet irradiation of polysulfone. Interestingly, SO_2 has been reported to be the major gas product in γ-irradiation[4,5] and thermal degradation[6,7] of polysulfone in vacuum.

High quantum yields for gas formation have been determined for the three systems evaluated. These values indicate photolytic instability. For comparison, the quantum yields for total gas are of the same order of magnitude as in polystyrene, and about an order of magnitude higher than in poly(methyl methacrylate).

G values have been previously reported for polysulfone (clear film). Brown and O'Donnell[4] reported an average *G* (total gas) of 0.04 for γ-irradiation. Davis et al.[3] reported an average *G* (total gas) of 0.01 for electron irradiation. Our value for initial *G* (total gas) for P1700 is approximately 0.03. *G* values (total gas) are higher for Fiberite 934 and Narmco 5208 [*G* (total gas) = 0.05 and 0.12, respectively] mainly because of a higher G_{H_2} (and a higher G_{CO_2} for Narmco 5208). However, all values are quite low relative to most polymers, indicating high electron radiation resistance. The lower *G* (total gas) for P1700 compared to the two epoxy systems indicates greater electron stability of P1700 resin, at least in terms of gas formation. Although, as a rule, higher radiation stability in terms of gas formation is reflected in higher radiation stability in terms of mechanical properties, this may not be true in this case, because P1700 is a linear polymer and its mechanical properties are likely to be more sensitive to molecular changes than Narmco 5208 and Fiberite 934 which are highly crosslinked thermosets.

GC/MS analyses of higher molecular weight compounds condensible at liquid nitrogen temperature resulted in the identification of a large number of products, particularly for ultraviolet exposed samples. These products were present only in trace quantities and did not contribute significantly to the total gas yield. The most important compounds identified in this group are shown in Table III for ultraviolet and electron exposed samples. Although a much greater variety of compounds were identified from ultraviolet exposed samples, there are remarkable similarities between the products obtained with ultraviolet and electron irradiation, indicating that similar free radical processes take place. The same observation was made earlier for the products identified by GC with a Porapak column.

A surprisingly large number of linear alkanes up to C_{16} have been identified, along with alkenes, cycloalkanes, and cycloalkenes. These compounds indicate that, although radiation attack of the benzene ring relative to the aliphatic portion of the polymers is not favored, decomposition of the benzene ring does take place under ultraviolet and electron irradiation. Hydrogen abstraction from the benzene ring is not energetically favored and is unlikely to occur. Phenyl radicals are certainly formed by main chain cleavage, but they are not expected to lead to decomposition of the ring. The most likely explanation is an attack of the benzene ring by hydrogen atoms to form cyclohexadienyl radicals. Formation of cyclohexadienyl radicals has been conclusively demonstrated by Lyons et al.[8] in a ESR study of γ-irradiated polysulfone, in which cyclohexadienyl radicals were detected together with phenoxy and phenylsulfone radicals. From cyclohexadienyl radicals, cycloalkenes and cycloalkanes can be readily formed by subsequent hydrogen attack. Quenching of cyclohexadienyl radicals may lead to the formation of cyclohexa-1,3-diene, which is known to rearrange under the effect of UV light to form hexa-1,3,5-triene.[9] Either this rearrangement or a direct cleavage of cyclohexadienyl radicals followed by recombination of hydrocarbon fragments is probably responsible for the formation of linear alkenes and alkanes.

Aromatic compounds identified by GC/MS include benzene, toluene, ethylbenzene, xylene, and several more in the case of ultraviolet irradiated polysulfone. Their formation can be explained by free radical mechanisms. Xylene must be present as residual solvent in P1700, because the amount of xylene detected from ultraviolet and electron irradiated P1700 samples is excessively high.

Formation of acetone is ascribed to the decomposition of isopropylbenzene hydroperoxide which is photolytically decomposed to acetone and phenol. From epoxy type systems, evolution of acetone cannot be readily explained. As in- arises from a double process of cleavage and hydrogen abstraction at the isopropylidene unit.

Formation of acetone is ascribed to the decomposition of isopropylbenzene hydroperoxide which is photolytically decomposed to acetone and phenol. From epoxy tube systems, evolution of acetone cannot be readily explained. As indicated in the case of CO_2 formation, formation of acetone confirms that oxygen plays a role in the photolytic process, in spite of the fact that the irradiations were conducted under high vacuum. Most likely, peroxidated groups were originally present in the polymer. Oxidative processes may also arise from the decomposition of SO_2 according to the mechanisms discussed previously.

A variety of sulfur compounds have been identified from ultraviolet irradiated

TABLE III
Ultraviolet and Electron Irradiation of Laminate Samples: Combined GC/MS Analysis of Evolved Products (OV-101 Column)

Material: Irradiation product	Total dose: 960 ESH P1700/C6000 (mol/cm^2 × 10^{12})	960 ESH 934/T300 (mol/cm^2 × 10^{12})	960 ESH 5208/T300 (mol/cm^2 × 10^{12})	10^9 rads P1700/C6000 (mol/g × 10^{10})	10^9 rads 934/T300 (mol/g × 10^{10})	10^9 rads 5208/T300 (mol/g × 10^{10})
Benzene	334	97.9	1190	13.4	0.13	2.32
Toluene	66.6	12.2	32.7	0.37	—	1.19
Xylene	554	0.19	4.03	8.06	—	—
Ethylbenzene	204	0.51	0.44	0.82	—	—
Chlorobenzene	8.3	—	—	2.5	—	—
Alkanes, open chain[a]	823	112	341	7.51	2.37	3.15
Alkenes, open chain[b]	721	8.93	24.9	—	—	—
Cyclohexane	215	3.96	14.9	—	0.16	—
Cyclohexene	285	0.26	0.7	—	—	—
Acetone	91.8	21.8	—	18.9	—	—
Propionitrile	—	0.37	—	—	—	—
Carbonyl sulfide	21.6	—	—	68.3	—	—
Carbon disulfide	9.7	3.04	2.33	—	—	—
Dimethylsulfide	—	9.43	19.3	—	—	—
Dimethyldisulfide	—	3.03	—	—	—	—
Methylethylsulfide	—	2.95	1.11	—	—	—

[a] Saturated linear and branched hydrocarbons (C_4–C_{16}).
[b] Unsaturated linear and branched hydrocarbons (C_4–C_{12}).

TABLE IV
Compressive Strength

Material	Exposure	Strength (MPa) (av of 3 Spec)
934/T300	Control	505
	UV exposed, 960 ESH	627
	Electron exposed, 10^9 rads	573
P1700/C6000	Control	365
	UV exposed, 960 ESH	253
	Electron exposed, 10^9 rads	418
5208/T300	Control	480
	UV exposed, 960 ESH	489
	Electron exposed, 10^9 rads	532

samples, such as carbonyl sulfide (COS), carbon disulfide (CS_2), dimethylsulfide (CH_3–S–CH_3), dimethyldisulfide (CH_3–S–S–CH_3), and methylethylsulfide (CH_3–S–C_2H_5). Formation of small quantities of COS were previously reported for electron irradiation,[3] γ-irradiation,[4] and UV irradiation[1] of polysulfone in vacuum. These sulfur compounds must arise from secondary reactions of SO_2. SO_2 must act as an oxidant, since the sulfur compounds identified by GC/MS have a lower oxidation number. As indicated earlier, SO_2 can undergo photochemical and radiochemical decomposition into SO and O_2; and SO can undergo disproportionation to SO_2 and elemental sulfur.[2] Elemental sulfur may react with CO to form COS, which in turn may decompose with formation of CS_2[10,11]:

$$CO + S \rightarrow COS$$

$$2COS \rightarrow CS_2 + CO_2$$

The absence of nitrogen containing compounds in the gas mixtures is quite remarkable. Nitrogen is present in Fiberite 934 and Narmco 5208 [4,4′-diaminodiphenyl sulfone (DDS) is used as hardener for these resins]. Only in the case of UV-exposed Fiberite 934 have traces of nitriles been identified. Ammonia or amines were not detected. This indicates good radiation stability for the portion of the molecule linking DDS to the epoxy system.

Chlorobenzene was detected in the ultraviolet and electron irradiation of P1700/C6000. Chlorobenzene arises from chlorophenyl end groups present in P1700 (which is prepared from 4,4′-dichlorodiphenylsulfone). Formation of chlorobenzene is an indirect proof of the occurrence of chain cleavage at C—S bonds. Likewise, benzene formation results from chain cleavage reactions taking place at random points in the polymer chain at both ends of the benzene ring.

Physical Testing

Compressive and flexural strength measurements have been conducted on control samples, ultraviolet exposed samples (960 ESH) and electron exposed samples (10^9 rads) of P1700/C6000, Fiberite 934/T300, and Narmco 5208/T300. Compressive strengths for these materials are presented in Table IV. With the exception of P1700/C6000, there is no evidence to indicate that the UV or electron

TABLE V
Flexural Strength

Material	Exposure	Strength (MPa) (avg of 3 Spec)
934/T300	Control	1370
	UV exposed, 960 ESH	1580
	Electron exposed, 10^9 rads	1560
P1700/C6000	Control	1100
	UV exposed, 960 ESH	710
	Electron exposed, 10^9 rads	850
5208/T300	Control	1870
	UV exposed, 960 ESH	2000
	Electron exposed, 10^9 rads	2020

exposed samples are different in strength from the control samples. Flexural test results are given in Table V. The behavior is essentially the same as that shown for compressive strength. The 934/T300 and 5208/T300 materials show no significant variation in strength. There may be flexural strength degradation in UV exposed P1700/C6000.

Dynamic Mechanical Analysis of Electron Exposed Samples

The dynamic mechanical behavior of Fiberite 934/T300 and Narmco 5208/T300 has been measured in the sample transverse direction. The loss modulus of electron irradiated samples (10^9 rads) and control samples are compared in Figures 1 and 2 for 934/T300 and 5208/T300, respectively. The loss modulus curves show that both 934/T300 and 5208/T300 have high temperature (α) and low temperature (β) transitions. The temperature at which these transitions occur (as measured by the temperature of the transition peak) appears to change as a result of electron irradiation, but the direction of the change is not the same for the two resins. According to the loss modulus plots, irradiation increases

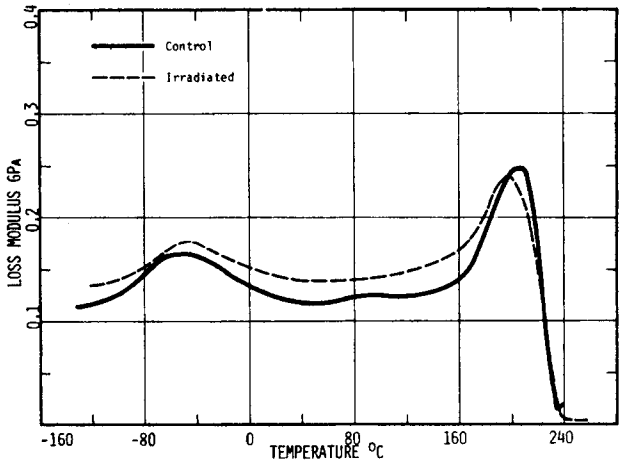

Fig. 1. Effect of electron irradiation (10^9 rads) on the loss modulus of Fiberite 934/T300: (—) control; (- - -) irradiated.

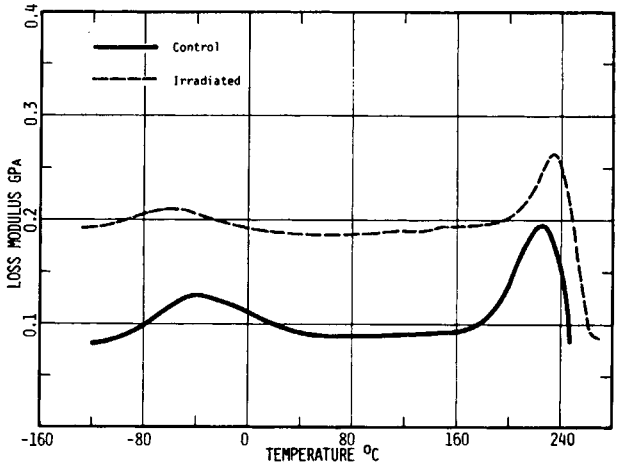

Fig. 2. Effect of electron irradiation (10^9 rads) on the loss modulus of Narmco 5208/T300: (——) control; (- - -) irradiated.

the α peak temperature in the case of 5208/T300, but decreases it for 934/T300. The increase in the α transition temperature of Narmco 5208 is probably related to evolution of hydrogen which was particularly high at 10^9 rads. (Polymers which are known to crosslink under the effect of radiation produce predominantly hydrogen as a byproduct.)

CONCLUSIONS

The composite materials evaluated have shown good electron radiation stability as indicated by low G values for gas formation and no evidence of mechanical property changes up to radiation doses of 10^9 rads. The same composites have shown poor stability to ultraviolet radiation in terms of quantum yields for gas formation. In terms of mechanical properties, no measurable changes have been detected up to 960 ESH, with the possible exception of P1700/C6000. Because of the high aromaticity of the matrix resins investigated, ultraviolet radiation is totally absorbed at the surface, and a "skin effect" is produced.

Quantitative analysis of volatile products evolved during radiation exposure has been found to be very useful for determining radiation stability. Gas formation in irradiated polymers reflects the occurrence of chain scission and crosslinking reactions, which are ultimately responsible for mechanical failure. The gas analysis technique is very sensitive and reveals changes occurring at the molecular level long before these become apparent in terms of physical property changes. Several free radical mechanisms of matrix degradation have been identified, and the radiation resistance of different matrices has been interpreted on the basis of their rates of gas evolution. Correlations between molecular effects of degradation (gas formation) and gross effects (changes in mechanical properties) have not been established because the radiation doses employed were insufficient to produce measurable physical property changes in the laminates tested. An increase in the T_g of 5208/T300 at 10^9 rads appears to be related to hydrogen formation, which is particularly high at this dose.

This work was conducted for NASA–Langley Research Center under Contract No. NASI-15469. The authors wish to acknowledge the cooperation and assistance of Mr. W. S. Slemp, the NASA-Langley Project Monitor.

References

1. B. D. Gesner and P. G. Kelleher, *J. Appl. Polym. Sci.*, **12,** 1199 (1968).
2. G. Nickless, Ed., *Inorganic Sulfur Chemistry*, Elsevier, New York, 1968, p. 374.
3. A. Davis, M. H. Gleaves, J. H. Golden, and M. S. Huglin, *Makromol. Chem.*, **129,** 63 (1969).
4. J. R. Brown and J. H. O'Donnell, *J. Appl. Polym. Sci.*, **19,** 405 (1975).
5. J. R. Brown and J. H. O'Donnell, *J. Appl. Polym. Sci.*, **23,** 2763 (1979).
6. A. Davis, *Makromol. Chem.*, **128,** 242 (1969).
7. W. F. Hale, A. G. Farnham, R. N. Johnson, and R. A. Clendining, *J. Polym. Sci A-1*, **5,** 2399 (1967).
8. A. R. Lyons, M. C. R. Symons, and J. K. Yandell, *Makromol. Chem.*, **157,** 103 (1972).
9. R. J. DeKock, N. G. Minard and E. Habinga, *Rec. Trav. Chem.*, **79,** 922 (1960).
10. J. R. Parkinson and H. H. Neville, *J. Chem. Soc.*, **1951,** 1230 (1951).
11. S. Oae, *Organic Chemistry of Sulfur*, Plenum, New York, 1977, p. 39.

Received February 11, 1983
Accepted June 29, 1983